18TH WORLD CONFERENCE ON EARTHQUAKE ENGINEERING
WCEE2024
MILAN

MILAN, ITALY
30TH JUNE - 5TH JULY 2024
www.wcee2024.it

ROLE OF HORIZONTAL TIMBER BANDS IN THE OUT-OF-PLANE BEHAVIOUR OF MASONRY STRUCTURES IN THE HIMALAYAS

U. Jain[1], M. Mirra[2], G. Ravenshorst[2] & F.Messali[3]

[1] TU Delft – Applied Mechanics, Delft, The Netherlands, u.jain-3@student.tudelft.nl

[2] TU Delft – Bio-Based Structures and Materials, Delft, The Netherlands

[3] TU Delft – Applied Mechanics, Delft, The Netherlands

Masonry structures occupy a significant share of the current building stock due to widespread material availability and cost-effectiveness. Regions with high seismicity, such as the Himalayas, have often developed a local seismic culture over the centuries. This has led to improved construction techniques providing an enhanced seismic performance, as evident from post-earthquake surveys in this area. In this framework, Bhatar is a building typology found in the greater Himalayan region, which features embedded horizontal timber bands in masonry walls, enhancing the box-behaviour and in turn avoiding their premature out-of-plane failure. This work aims to quantify the improvement of the out-of-plane performance of masonry walls because of the presence of horizontal timber bands. In order to achieve this research objective, numerical analyses were conducted in DIANA FEA finite element software starting from the few experimental results on this building typology available in the literature. These were used to calibrate the properties of masonry, which was represented as a homogeneous isotropic continuum, with nonlinearities taken into account by means of a total strain rotating crack model. Firstly, a U-shaped masonry wall having the same geometry and boundary conditions as the experimental tests was simulated using a 3D modelling approach. Non-linear static analyses were performed and very good agreement was obtained with the results from the literature. On this basis, the calibrated numerical model was then employed to conduct sensitivity analyses considering varying factors, such as masonry material properties, geometry, opening configurations, timber section sizes and properties. The outcomes of this extensive study show a considerable improvement in the out-of-plane response of the masonry walls in the presence of horizontal timber bands. Given the limited research conducted on the Bhatar building typology in the past, this work constitutes a further step towards a better understanding of the behaviour of Himalayan masonry structures under earthquakes, promoting more effective seismic risk reduction strategies. This improved understanding into timber's role in imparting greater seismic resilience to masonry structures can inform better maintenance, conservation and preservation of heritage and historical masonry structures in the Himalayas.

1 Introduction

Masonry is one of the most prominent construction materials humans have used to house themselves, with the earliest forms of masonry being reported as far as 7,500 years ago. Despite the prolific adoption of reinforced concrete and steel as building materials in the 20th and 21st centuries, brick and stone remain prevalent as walling materials due to local availability in remote regions. As a result, most culturally and traditionally significant historical structures are built using masonry. The Himalayan region in the Indian

subcontinent, is an example of such a remote area, with a high frequency of earthquakes (Singh et al. 2015),. The region has experienced high casualties in the past, with predictions of a death toll well over 200,000 from a strong earthquake in the future due to a higher population density (Wyss et al. 2018). Masonry continues to occupy a significant portion of the current building stock of this region (Parajuli and Kiyono 2015, Gautam et al. 2018, Gautam and Chaulagain 2016, Sharma et al. 2022).

Masonry constituents – mortar and units – have much larger compressive strength than tensile strength. Consequently, masonry resists gravity loads well, but it is vulnerable to imposed lateral loads. Most failure mechanisms of unreinforced masonry (URM) can be categorized into in-plane (IP) or out-of-plane (OOP) failures. IP failure modes (rocking, toe-crushing and shear failure) are influenced by compressive, tensile and shear strength of the masonry, vertical load on the wall, and aspect ratio. The ability of the diaphragms to adequately connect the orthogonal walls and the extent of supported edges are some of the factors affecting OOP failure (Vlachakis et al. 2020, Vaculik 2012, Mirra and Ravenshorst 2021, Mirra et al. 2022). Both IP and OOP failures have been observed in the Himalayan region during the post-earthquake surveys (Naseer et al. 2010, Gautam and Chaulagain 2016, Shakya and Kawan 2016, Adhikari and D'Ayala 2020, Rai et al. 2015, Javed et al. 2006). Regions with high seismic activity usually develop a local seismic culture (Karababa and Guthrie 2007, Bostenaru Dan 2014, Langenbach 1989), and timber is commonly adopted to reinforce the masonry and resist tension and bending forces (Vasconcelos et al. 2015, Mirra et al. 2023). In this framework, *Bhatar* is a building typology prevalent in the Himalayas, featuring horizontal timber bands embedded in stone (or brick) masonry to provide the structure with better resistance to out-of-plane movements.

Quasi-static in-plane tests on single walls (Aranguren et al. 2020, Wang et al. 2019b, Yadav et al. 2021) and dynamic tests on full structures (Wang et al. 2019a, Yadav et al. 2023, Mouzakis et al. 2018) have highlighted the positive impact of timber bands on masonry by confining cracks, enhancing ductility and energy dissipation by distributing loads, in turn enhancing structural integrity and preventing total collapse of masonry structures. Out-of-plane pushover tests conducted by Murano et al. (2019) found a 52% increase in the lateral resistance of a masonry wall when reinforced with timber bands at corners. While experimental investigations are expensive, numerical modelling allows for more convenient exploration of behaviour of masonry. However, the accuracy of the numerical studies rely heavily on the availability of precise values material properties and thorough calibration. For this reason, the experimental and numerical study by Murano et al. (2019) was chosen as a benchmark for this investigation. The study starts from the actual geometry and material properties, and is then completed by investigating the performance of the wall strengthened with continuous timber bands. Finally, a sensitivity study is conducted to assess the influence of aspect ratio and pre-compression on the response of the masonry wall.

2 Finite element model

2.1 Literature study

Numerical characterisation of masonry can be done using four predominant approaches - block-based models, continuum models, macroelement models, geometry-based models (D'Altri et al. 2020). However, the focus here will be on Finite Element Analysis (FEA) within which, micromodelling and macromodelling emerge as the two major approaches (Lourenco 2009). The former models explicitly the discrete components (brick and mortar), as well as the bond interaction at the interface between the two materials, while the latter idealises masonry as a composite material. In this context, few researchers have undertaken numerical investigation of masonry buildings with horizontal timber bands through FE (finite element) models. Khadka et al. (2023) used macromodelling approach and employed Engineering masonry model (Schreppers et al. 2016) with a combined cracking, crushing, shearing material behaviour to conduct FE analysis of a *Sherpa* house in Nepal. The study found an improvement of 73.5% in lateral strength of an unreinforced stone masonry structure upon reinforcement with buttresses, timber bands and roof-to-wall connections. Lourenço et al. (2019) conducted a seismic assessment to find that after strengthening, the retrofitted Church Kuno Tambo (in Peru) met the performance criteria and local seismic demand, achieved through better distribution of seismic load between lateral and transversal walls and increased energy dissipation. Ortega et al. (2018) compared the performance of a two-storey rammed earth structure before and after retrofitting to find that the inclusion of timber laces almost tripled the maximum capacity and delayed the crack propagation.

Murano et al. (2019) also conducted a pushover test of a return wall with and without timber bands. A 3D FE model with macro-modelling approach was considered and the Total Strain Rotating Crack model (DIANA FEA

B.V. 2021) was used to define the non-linear behaviour of stone masonry. The authors calibrated the linear and non-linear properties from the results of the sonic tests and experimental out-of-plane tests, respectively. The numerical models were able to attain maximum load values close to the experimental ones, but post-peak, showed sharper softening compared to the experimental curve.

2.2 Elements and mesh

A tetrahedron 3D element based on quadratic interpolation, leading to a twenty node CHX60 element (DIANA FEA B.V. 2021), was chosen to model concrete, masonry and timber elements using a regular 2×2×2 integration scheme. The connection between the concrete base and the floor was modelled using three-dimensional plane quadrilateral interface elements - CQ48I, based on quadratic interpolation and using 3×3 Newton-Cotes integration scheme (DIANA FEA B.V. 2021). The average mesh size was 0.10 m and 0.05 m for the masonry and timber elements, respectively.

2.3 Geometry

The dimensions of the single components of the return wall tested by Murano et al. (2019) are listed in Table 1. Such data was used to define the geometry of the numerical model constructed in DIANA, as displayed in Figure 1.

Table 1. Dimensions of the masonry wall according to the experimental setup by Murano et al. (2019).

Component	**Length** (m)	**Width** (m)	**Height** (m)
Frontal wall	2.250	0.300	1.350
Lateral wall	1.000	0.300	1.350
Longitudinal timber beam	0.700	0.050	0.035
Transversal cross piece	0.200	0.035	0.025

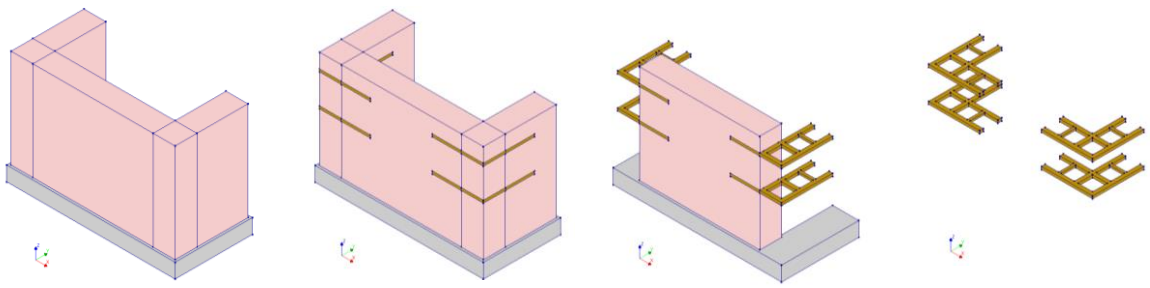

(a) (b) (c) (d)

Figure 1. Masonry walls model – (a) Unreinforced masonry; (b) and (c) Timber-reinforced masonry; (d) Timber laces.

2.4 Material model

A smeared crack approach using the Total Strain Rotating Crack model (TSRCM) was used to model the non-linear behaviour of stone masonry. This model is appropriate to analyse the cracking and the crushing response of stone masonry. Exponential softening and a parabolic curve are selected to describe the tensile and compressive behaviour of the masonry, respectively, consistently with the model described in Murano et al. (2019). Since no damage to the timber elements was reported, timber and concrete are modelled via linear elastic elements. However, the stresses developed in the timber elements are assessed against the material strength in the post-processing phase.

2.5 Material properties

The material properties are taken from the study conducted by Murano et al. (2019) and listed in Table 2.

Table 2. Material properties of masonry, timber and concrete, Murano et al. (2019).

Element	Poisson ratio	Density	Young's Modulus	Strength		Fracture energy	
				Comp.	Tensile	Comp.	Tensile
		kg/m^3	MPa	MPa	MPa	N/m	N/m
Unreinforced masonry	0.39	2495	3600	3.6	0.07	5760	12
Timber-reinforced masonry	0.25	2482	2974	2.97	0.07	4760	12
Timber	0.2	600	10000				
Concrete	0.2	2400*	31000				

*Density of concrete assumed

2.6 Loads

Apart from self-weight, two load sets were imposed on the wall as seen in Figure 2. A uniformly distributed vertical load was applied on the lateral walls to simulate the experimental vertical load representing the weight of a heavy timber roof. This load was firstly applied incrementally, and then maintained constant. Secondly, the horizontal load applied in the experiment through the airbag was simulated by a uniformly distributed horizontal load on the rear façade of the frontal wall. This load was applied incrementally in a second phase of the analysis.

(a) (b)

Figure 2. Loads applied – (a) Roof load to the lateral walls, and (b) Pushover load to the frontal wall.

2.7 Interaction between structural components

The concrete base and the timber bands were considered to be fully connected with the masonry wall. The interface between the concrete base and the floor (Figure 3b) has been modelled using the boundary interface elements properties provided by Murano et al. (2019), listed in Figure 3a. Due to the geometry of the timber bands that allows for interlocking with the masonry stones, full connection between timber and masonry is assumed.

Model	Normal Stiffness (N/mm^3)	Tangential Stiffness (N/mm^3)
Unreinforced masonry	0.992	0.397
Timber-reinforced masonry	0.640	0.257

(a)

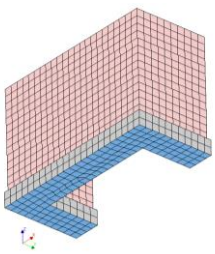

(b)

Figure 3. a) Interface stiffness between concrete base and floor by Murano et al. (2019), and b) Interface between concrete base and floor

2.8 Analyses plan

The numerical simulations were conducted within the software DIANA FEA (DIANA FEA B.V. 2021), which supplies multiple incremental-iterative solution procedures for nonlinear analysis: among those, two iterative techniques were adopted: Regular Newton-Raphson and Secant Quasi-Newton. For the former, the stiffness

relation is evaluated for every iteration based on the previous prediction making it time-consuming, but achieving convergence within fewer iterations. The latter depends on the out-of-balance force vectors from the previous iteration for approximation of the solution, eliminating the need of setting up a stiffness matrix with every iteration. The number of iterations was set at 100. Additionally, arc-length control was used to provide stable solution in the post-peak phase. Convergence criteria for either force or displacement with a convergence norm of 1% were prescribed.

It should be noticed that two different models were selected to describe the reduction of Poisson's ratio after cracking: a) No reduction, and b) Damage based reduction. For the former the behaviour under lateral cracking remains the same, while the latter decreases Poisson's ratio, resulting in increased damage as cracking progresses. The combination between iterative techniques and Poisson's ratio reduction models is reported in Table 3.

Table 3. Variations of the two models.

Model	Wall	Iterative technique	Poisson's ratio reduction model
Model U1	Unreinforced	Regular Newton-Raphson	Damage-based reduction
Model T1	Timber-reinforced		
Model U2	Unreinforced	Secant Quasi-Newton	No reduction
Model T2	Timber-reinforced		

3 Results

3.1 Base shear capacity

The shear force at base computed for each load-step of the performed analyses was plotted against the displacements obtained for the control node (top-mid section of the frontal wall) to derive pushover curves. The comparison of the pushover curves with those found in the literature can be seen in Figure 4. The maximum lateral resistance achieved in both numerical models (45.77 kN and 45.68 kN) is approximately equal to the experimental value (45.64 kN). For timber-reinforced masonry (62.51 kN and 65.95 kN), the same value is 7-9% smaller than the experimental value (68.92 kN). The pushover curves for both numerical models correspond closely to each other with a slightly sharper drop in capacity after peak force for the Model T1. The timber-reinforced masonry has a maximum lateral force capacity around 40% higher than that computed for the unreinforced masonry specimen, consistently with the experimental results.

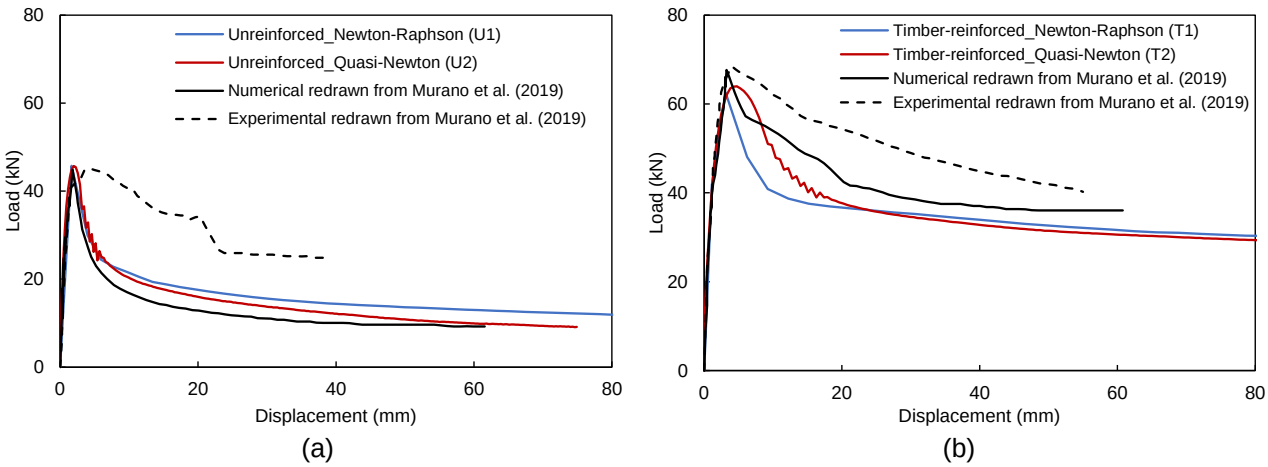

Figure 4. Pushover curve comparison with literature – a) Unreinforced, and b) Timber-reinforced masonry

3.2 Displacement contours

Figure 5 compares the contour plots for the OOP displacements obtained through the pushover analyses against those obtained from experimental and numerical investigations conducted by Murano et al. (2019). The comparison reveals reasonable correspondence with the benchmark studies. The asymmetry in

experimental displacements cannot be replicated by macro numerical models as the geometry of each stone is not modelled explicitly. Moreover, since macromodelling is a continuum approach, the cracks are assumed to *smear* evenly across the surface of the wall and does not have irregularities related to construction, mortar joints, thickness, etc. This leads to the difference in the response of the so-called *stronger* parts of the wall to the *weaker* parts. There is a distinct contrast between the failure mechanisms observed from the displacement contours of the two models. While Models U2 and T2 are able to achieve the failure mechanism of horizontal flexure in both the unreinforced and timber-reinforced frontal walls, Model U1 fails through separation of orthogonal walls in the unreinforced masonry. This separation is avoided in the timber-reinforced masonry Model T1, and is attributed to the presence of the timber laces. Since the laces are present only at the corners, the failure is concentrated at the centre portion of the frontal wall.

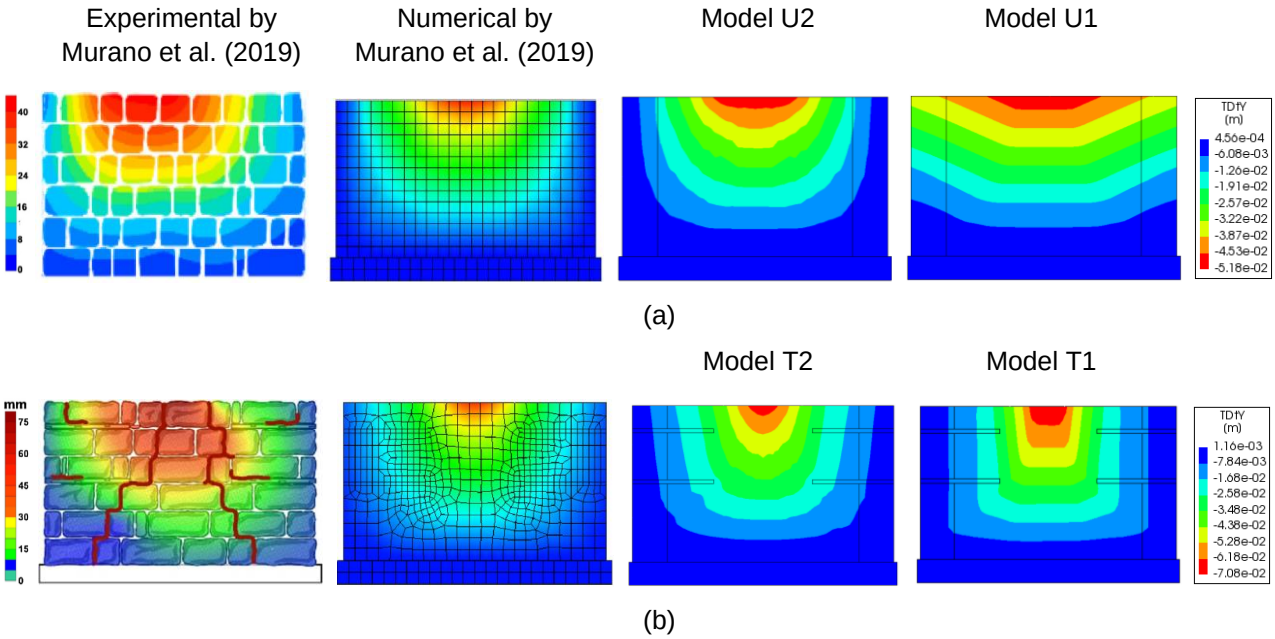

Figure 5. Displacement contours: (a) Unreinforced masonry, and (b) Timber-reinforced masonry

The difference between the two models in simulating varying failure mechanisms for the unreinforced case is depicted in Figure 6. While Model U1 exhibits separation of the frontal wall from the returning walls; Model U2 shows horizontal bending under out-of-plane loading conditions.

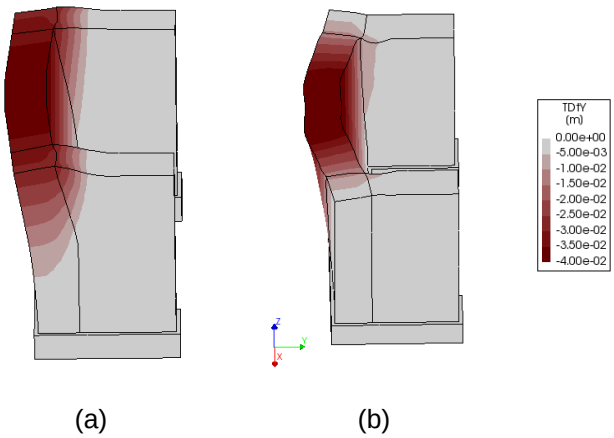

Figure 6. Side view of displacement in Y direction: (a) Model U1, (b) Model U2

3.3 Crack patterns

The accuracy of the models to describe the damage evolution is assessed by plotting principal crack widths and the variation between the two models are compared with experimental cracking patterns by Murano et al. (2019) in Figure 7. The crack plots are taken at 40 and 57 mm displacement of the top node for unreinforced

and timber-reinforced masonry, respectively. Models U1 and T1 simulate the experimental crack pattern accurately, displaying localised damage evolution at distinct locations, including the horizontal crack in the rear façade of the frontal wall, two courses from the bottom of the masonry wall and the diagonal crack in the frontal wall. The experimental crack on the outside wythe of the lateral wall is also well predicted. Models U2 and T2 also provide an adequate depiction of the experimental diagonal cracks on the front façade, albeit with more smearing of the cracks. However, they fail to represent any cracks on the lateral wall. Both models depict most significant cracking at two locations – (i) base of the frontal wall at the rear façade, due to overturning action, and (ii) corner connection of frontal and lateral walls, due to separation action. The vertical crack at the corner is also represented. Model U2 is able to simulate the cracks well for unreinforced masonry though with more distribution of the cracks across the surface, in contrast to better localisation achieved by Model U1. Another local crack in the experiment simulated precisely by the Model T1 is the clear horizontal crack visible at mid-height of the rear façade for timber-reinforced masonry.

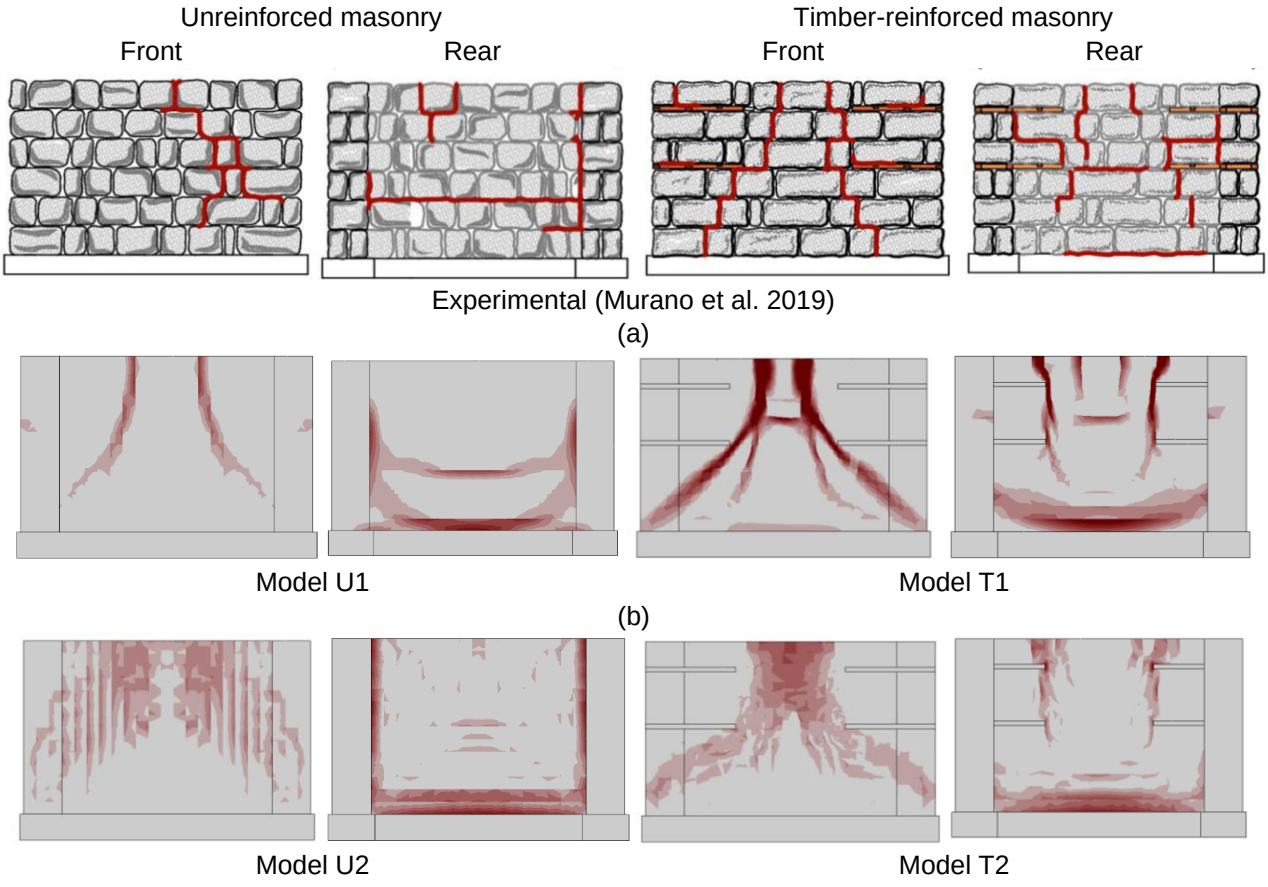

Figure 7. Crack patterns: (a) Experimental by Murano et al. (2019), (b) Numerical by Model U1 and T1, and (c) Numerical by Model U2 and T2.

4 Sensitivity study

4.1 Connected timber bands

A Bhatar building presents rarely discontinuous timber elements. On the contrary, the timber braces are connected throughout the length of the wall. Therefore, for the performance of a model with connected timber braces (Figure 8) was assessed. All the other parameters were retained from Model T2. In the updated model, the timber bands join throughout the frontal wall, and also extend to the end of the lateral walls. The cross beams connecting the parallel timber beams have similar spacing as in the previous models.

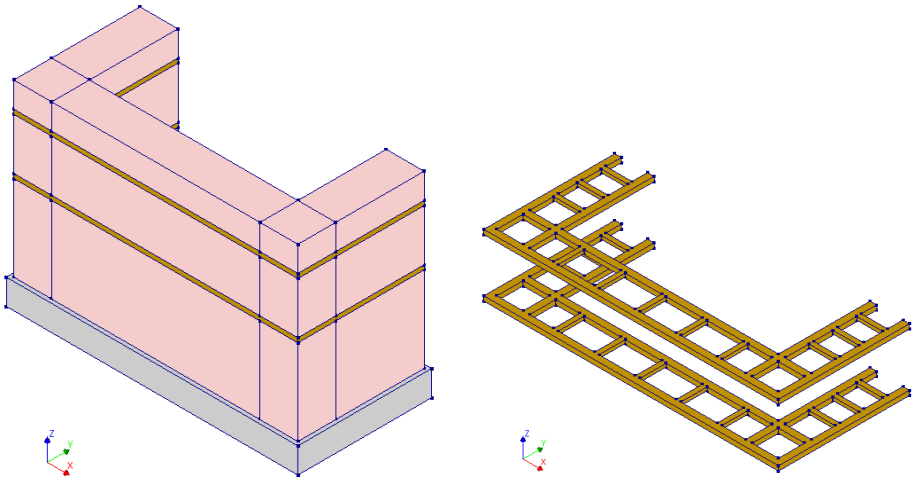

(a) (b)

Figure 8. (a) Numerical model for connected timber bands, and (b) timber laces

For seismic design, Eurocode 8 (EN 1998) specifies limit states for design and assessment of structures. Two limit states are considered in this study: the Severe Damage Limit State (SDLS), associated with the lateral drift corresponding to the out-of-plane peak load, and the Near Collapse Limit State (NCLS) – associated with the lateral drift corresponding to the 20% reduction of strength with respect to the peak value. The pushover curves in Figure 9 show a remarkable increase in the lateral resistance for walls with connected bands, along with a noticeable drop of force (15%) after the maximum load is attained. However after the initial softening, the force reduction is rather gradual, predicting higher ductility than for the case of discontinuous bands. While the drift capacity remained similar (0.35% and 0.38%) for both models at SDLS; at NCLS, the wall with connected bands showed a much higher drift capacity (1.5%) compared to that (0.69%) computed for the wall with discontinuous timber bands.

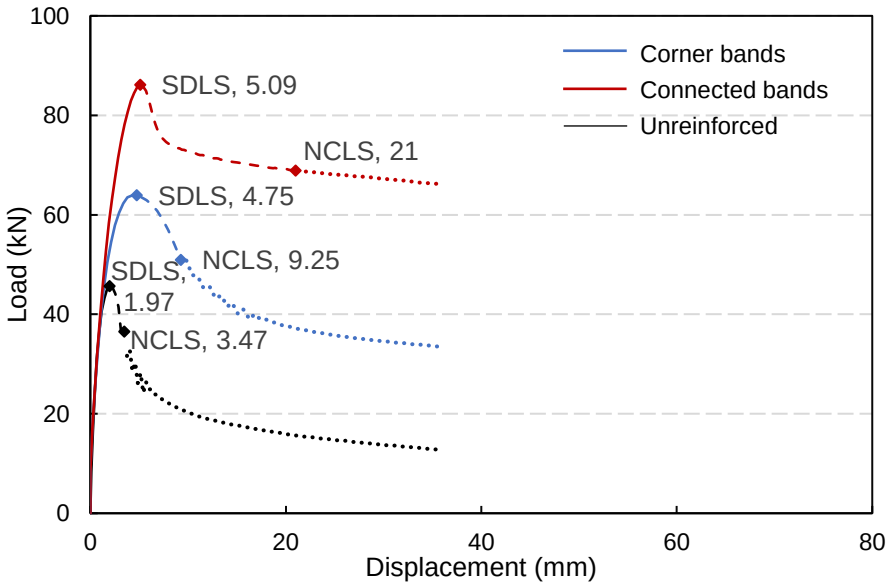

Figure 9. Load-displacement curve comparison: Bands at corners vs connected bands

The difference between the resistance of unreinforced and timber-reinforced masonry can be explained by assessing the stresses generated in the timber laces and comparing them to the stresses in the masonry. To this end, the tensile stresses (SXX) at the bottom row of the top timber lace on the front façade are compared to the stresses in masonry in Figure 10. The relative location of the ninety-one nodes chosen for stresses is highlighted, and the stresses are considered at the Near Collapse Limit State (NCLS). The OOP displacements of timber lace and masonry at NCLS are also compared. The figure illustrates that the stresses in masonry

remain below its tensile strength of 0.074 MPa. However, the stresses in timber at NCLS are already exceeding 6 N/mm^2, but are lower than the design bending strength of 18.46 N/mm^2 for the D24 strength class, here assumed as it relates closely to the material properties of the timber used in the experiments. On a local level, the stresses in timber laces are high at the location of the cross beams and low at the location between the cross beams. This is attributable to the better connection, and hence, better redistribution of stresses between the inner and the outer longitudinal timber section due to the presence of cross beams. On a global level, the stresses, expectedly, are minimum at the ends near the lateral walls and maximum at the mid-section of the frontal façade wall, mimicking the bending profile of the displacement of the band.

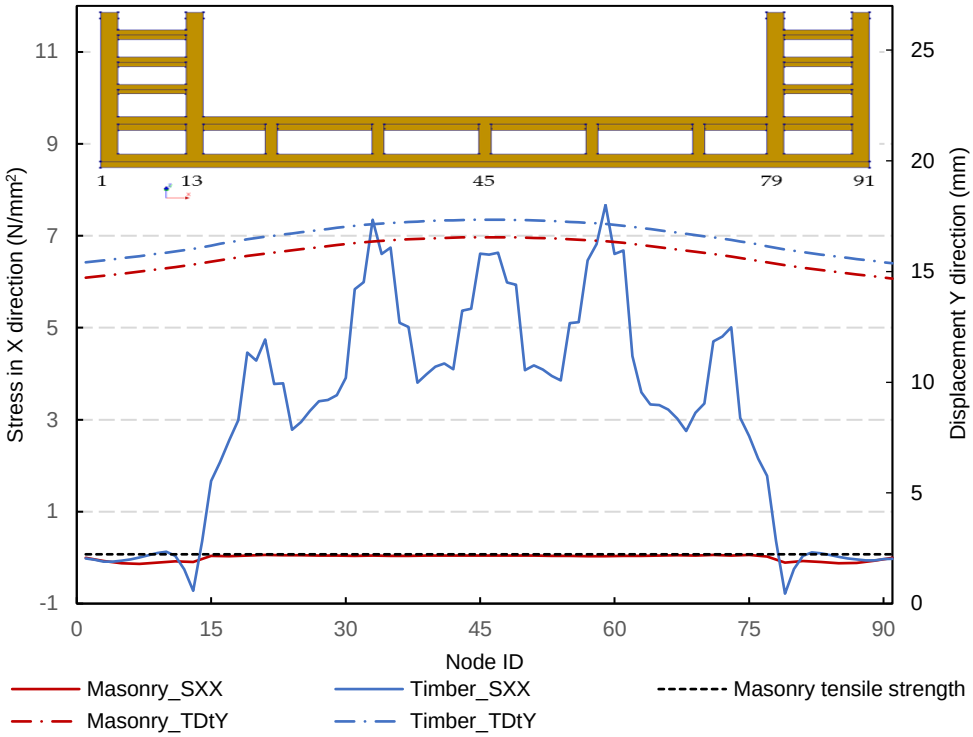

Figure 10. Stresses in X direction and displacement in Y direction for timber and masonry at NCLS

4.2 Influence of aspect ratio and pre-compression

Past experimental campaigns have found that the masonry tensile strength and the number of horizontal timber bands are the primary factors affecting the out-of-plane performance of a wall. However, additional experimental investigation on the influence of other parameters would be expensive and time-consuming. To this end, the calibrated numerical model proposed in this work is used to assess the influence of two factors, aspect ratio and pre-compression level.

The influence of the aspect ratio (length to height) of the wall was explored by varying the ratio between 1.0 and 2.0 for four models. The height is maintained constant, as shown in Figure 11. The load-displacement curves (Figure 12a) exhibit a trend in which the longer frontal walls demonstrate larger force capacity than the shorter walls.

Also two variations of the pre-compression level are considered. Half and the double of the experimental value (0.1 N/mm^2) are considered: 0.05 N/mm^2 and 0.2 N/mm^2, respectively. The former is representative of the actual weight of a heavy timber roof, while the latter denotes the pre-compressive load resulting from the overburden of more than one floors on masonry walls at lower levels. Figure 12b indicates the high sensitivity of the behaviour of the wall to the vertical compressive load on the lateral walls.

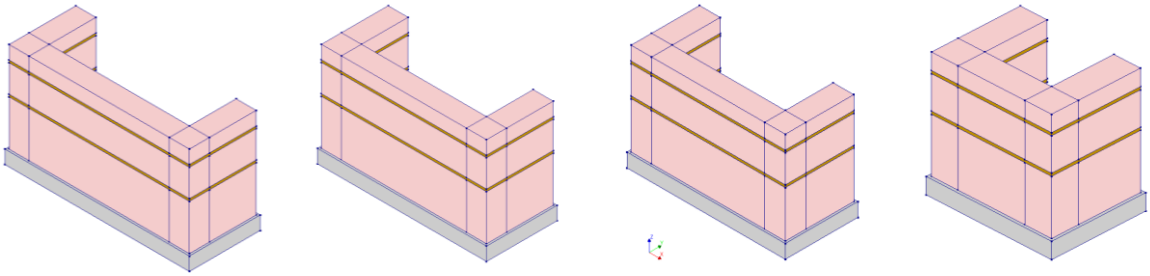

(a) (b) (c) (d)

Figure 11. Aspect ratio: (a) 2.0, (b)1.83, (c) 1.67, (d) 1.0

The maximum base shear force increased by 37% upon doubling the pre-compression and reduced by 18% upon halving it, suggesting an almost linear relationship between the pre-compression and force capacity. Similar relationship has been found in previous studies on the effect of precompression on unreinforced masonry subjected to out-of-plane two-way bending (Chang et al. 2021). However, a larger set of analysis results is needed to arrive at more certain conclusion. The difference between peak and residual force and force also decreases with the increasing pre-compression.

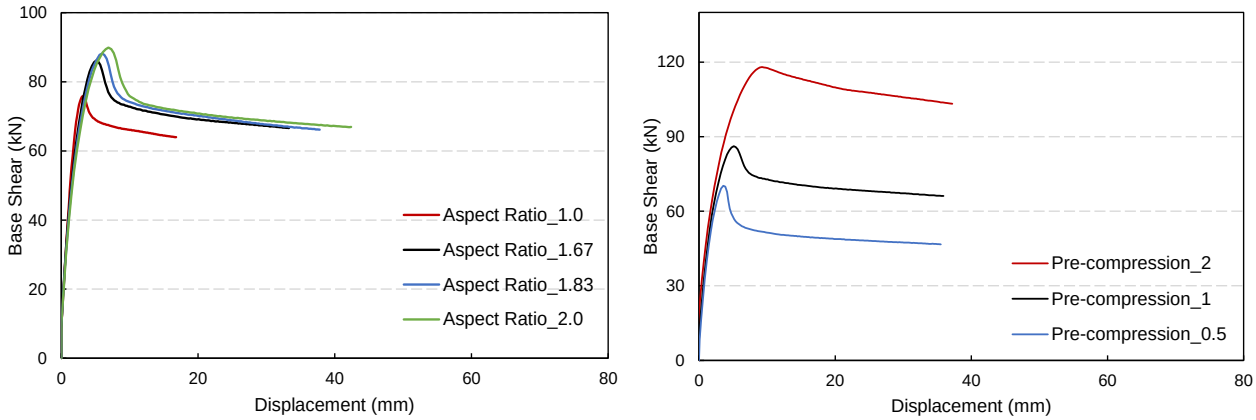

Figure 12. Sensitivity study: a) Aspect ratio, and b) Pre-compression level

5 Conclusions

This paper presents the results of a numerical study conducted on U-shaped masonry walls with horizontal timber bands, representative of the Bhatar building typology, typical of the Himalayan region. A macromodelling approach was used, and the analyses performed within the finite element software package DIANA FEA. Two models with varying iterative techniques were analysed, with one of them also accounting for lateral influence of cracking. The results were validated against experimental tests found in literature. While numerical models were effective at approximating experimental pre-peak behaviour and the peak loads, they predicted sharper post-peak softening compared to experimental observations.

The results of the simulations, in line with those of the experiments, show that the integration of timber bands in masonry increased the lateral resistance by 40% (at Severe Danage Limit State) and the displacement capacity by 49% (at Near Collapse Limit State), preventing, or at least, delaying collapse. Timber reinforcement also provided higher residual strength (35.5 kN compared to 14.13 kN for the unreinforced specimen), suggesting a larger potential for safety against sudden collapse.

Additional analyses were conducted to simulate walls with timber bands connected through the front wall (subjected to out-of-plane load). In this conditions, the wall showed a further 35% increase of load capacity than the wall with discontinuous timber bands (located only at the corners). This configuration substantially increased also the ductility of the wall, with 7% and 127% increase in the drift capacity by Severe Damage Limit State and Near Collapse Limit State, respectively.

Overall, this research underscores the vital role of horizontal timber bands in enhancing the seismic response of masonry structures, especially in the earthquake-prone Himalayan region, where Bhatar buildings are

erected. The integration of timber not only enhances the resistance and ductility of the structures but also significantly changes the failure mechanisms, leading to safer outcomes during seismic events. Further research is suggested in discretising the masonry to capture the frictional behaviour of timber-masonry interface and timber-to-timber connections in detail, which could potentially explain even more robust construction methodologies for seismic regions.

6 References

Adhikari, R. K. & D'Ayala, D. 2020. 2015 Nepal earthquake: seismic performance and post-earthquake reconstruction of stone in mud mortar masonry buildings. *Bulletin of Earthquake Engineering,* 18**,** 3863-3896.

Aranguren, J., Vieux-Champagne, F., Duriez, M. & Aubert, J.-E. 2020. Experimental analysis of timber inclusions effect on paraseismic behavior of earth masonry walls. *Engineering Structures,* 212**,** 110429.

Bostenaru Dan, M. 2014. Timber Frame Historic Structures and the Local Seismic Culture—An Argumentation. *Earthquake hazard impact and urban planning.* Springer.

Chang, L.-Z., Rots, J. G. & Esposito, R. 2021. Influence of aspect ratio and pre-compression on force capacity of unreinforced masonry walls in out-of-plane two-way bending. *Engineering Structures,* 249**,** 113350.

D'Altri, A. M., Sarhosis, V., Milani, G., Rots, J., Cattari, S., Lagomarsino, S., Sacco, E., Tralli, A., Castellazzi, G. & de Miranda, S. 2020. Modeling strategies for the computational analysis of unreinforced masonry structures: review and classification. *Archives of computational methods in engineering,* 27**,** 1153-1185.

Gautam, D. & Chaulagain, H. 2016. Structural performance and associated lessons to be learned from world earthquakes in Nepal after 25 April 2015 (MW 7.8) Gorkha earthquake. *Engineering Failure Analysis,* 68**,** 222-243.

Gautam, D., Chaulagain, H., Rupakhety, R., Adhikari, R., Neupane, P. & Rodrigues, H. 2018. Vernacular masonry construction in Nepal: History, dynamics, vulnerability and sustainability. *Masonry: design, materials and techniques. Nova Science Publishers Inc., New York*.

Javed, M., Naeem, A., Penna, A. & Magenes, G. Behavior of masonry structures during the Kashmir 2005 earthquake. Proc. Of the First European Conference on Earthquake Engineering and Seismology, Geneva, Switzerland, Paper, 2006.

Karababa, F. & Guthrie, P. 2007. Vulnerability reduction through local seismic culture. *Technology and Society Magazine, IEEE,* 26**,** 30-41.

Khadka, S. S., Acharya, S., Acharya, A. & Veletzos, M. J. 2023. Enhancement of Himalayan irregular stone masonry buildings for resilient seismic design. *Frontiers in Built Environment,* 9.

Langenbach, R. 1989. Bricks, mortar and earthquakes. *Apt Bulletin,* 31**,** 31-43.

Lourenco, P. 2009. Recent advances in Masonry modelling: micromodelling and homogenisation. *Multiscale Modeling in Solid Mechanics: Computational Approaches*.

Lourenço, P. B., Ciocci, M. P., Greco, F., Karanikoloudis, G., Cancino, C., Torrealva, D. & Wong, K. 2019. Traditional techniques for the rehabilitation and protection of historic earthen structures: The seismic retrofitting project. *International Journal of Architectural Heritage,* 13**,** 15-32.

Mirra, M., Gerardini, A., Ghirardelli, S., Ravenshorst, G. & van de Kuilen, J.-W. 2023. Combining Architectural Conservation and Seismic Strengthening in the Wood-Based Retrofitting of a Monumental Timber Roof: The Case Study of St. Andrew's Church in Ceto, Brescia, Italy. *International Journal of Architectural Heritage***,** 1-21.

Mirra, M. & Ravenshorst, G. 2021. Optimizing seismic capacity of existing masonry buildings by retrofitting timber floors: Wood-based solutions as a dissipative alternative to rigid concrete diaphragms. *Buildings,* 11**,** 604.

Mirra, M., Ravenshorst, G., de Vries, P. & Messali, F. 2022. Experimental characterisation of as-built and retrofitted timber-masonry connections under monotonic, cyclic and dynamic loading. *Construction and Building Materials,* 358**,** 129446.

Mouzakis, C., Adami, C.-E., Karapitta, L. & Vintzileou, E. 2018. Seismic behaviour of timber-laced stone masonry buildings before and after interventions: shaking table tests on a two-storey masonry model. *Bulletin of Earthquake Engineering,* 16**,** 803-829.

Murano, A., Ortega, J., Vasconcelos, G. & Rodrigues, H. 2019. Influence of traditional earthquake-resistant techniques on the out-of-plane behaviour of stone masonry walls: Experimental and numerical assessment. *Engineering Structures,* 201.

Naseer, A., Khan, A. N., Hussain, Z. & Ali, Q. 2010. Observed seismic behavior of buildings in northern Pakistan during the 2005 Kashmir earthquake. *Earthquake Spectra,* 26**,** 425-449.

Ortega, J., Vasconcelos, G., Rodrigues, H. & Correia, M. 2018. Assessment of the efficiency of traditional earthquake resistant techniques for vernacular architecture. *Engineering Structures,* 173**,** 1-27.

Parajuli, R. R. & Kiyono, J. 2015. Ground Motion Characteristics of the 2015 Gorkha Earthquake, Survey of Damage to Stone Masonry Structures and Structural Field Tests. *Frontiers in Built Environment,* 1.

Rai, D., Singhal, V., Selvaraj, B. R. & Sagar, L. 2015. Performance of Residential Buildings during the M 7.8 Gorkha (Nepal) Earthquake of 25 April 2015. *Current Science,* 109**,** 2126.

Schreppers, G., Garofano, A., Messali, F. & Rots, J. 2016. DIANA validation report for masonry modelling. *DIANA FEA report*.

Shakya, M. & Kawan, C. K. 2016. Reconnaissance based damage survey of buildings in Kathmandu valley: An aftermath of 7.8Mw, 25 April 2015 Gorkha (Nepal) earthquake. *Engineering Failure Analysis,* 59**,** 161-184.

Sharma, A. K., Kumar, A. & Sarhosis, V. Evaluating the Seismic Performance of Domestic and Historical Masonry Structures in Himachal Pradesh Region of India. *In:* KOLATHAYAR, S. & CHIAN, S. C., eds. Recent Advances in Earthquake Engineering, 2022// 2022 Singapore. Springer Singapore, 477-490.

Singh, Y., Lang, D. H. & Narasimha, D. Seismic risk assessment in hilly areas: case study of two cities in Indian Himalayas. Proc. SECED 2015 Conference: Earthquake Risk and Engineering towards a Resilient World, 2015. 9-10.

User's Manual - Release 10.5. 2021. *In:* FERREIRA, D. (ed.) *DIANA - Finite Element Analysis, DIsplacement method ANalyzer.* Delft, The Netherlands: DIANA FEA BV.

Vaculik, J. 2012. *Unreinforced masonry walls subjected to out-of-plane seismic actions.*

Vasconcelos, G., Lourenço, P. B. & Poletti, E. 2015. An Overview on the Seismic Behaviour of Timber Frame Structures. *In:* RUGGIERI, N., TAMPONE, G. & ZINNO, R. (eds.) *Historical Earthquake-Resistant Timber Frames in the Mediterranean Area.* Cham: Springer International Publishing.

Vlachakis, G., Vlachaki, E. & Lourenço, P. B. 2020. Learning from failure: Damage and failure of masonry structures, after the 2017 Lesvos earthquake (Greece). *Engineering Failure Analysis,* 117.

Wang, M., Liu, K., Guragain, R., Shrestha, H. & Ma, X. 2019a. Shake table tests on the two-storey dry-joint stone masonry structures reinforced with timber laces and steel wires. *Bulletin of Earthquake Engineering,* 17**,** 2199-2218.

Wang, M., Liu, K., Lu, H., Shrestha, H., Guragain, R., Pan, W. & Yang, X. 2019b. Increasing the lateral capacity of dry joint flat-stone masonry structures using inexpensive retrofitting techniques. *Bulletin of Earthquake Engineering,* 17**,** 391-411.

Wyss, M., Gupta, S. & Rosset, P. 2018. Casualty Estimates in Repeat Himalayan Earthquakes in India. *Bulletin of the Seismological Society of America,* 108**,** 2877-2893.

Yadav, S., Damerji, H., Keco, R., Sieffert, Y., Crété, E., Vieux-Champagne, F., Garnier, P. & Malecot, Y. 2021. Effects of horizontal seismic band on seismic response in masonry structure: Application of DIC technique. *Progress in Disaster Science,* 10**,** 100149.

Yadav, S., Sieffert, Y., Vieux-Champagne, F., Malecot, Y., Hajmirbaba, M., Arléo, L., Crété, E. & Garnier, P. 2023. Shake table tests on 1:2 reduced scale masonry house with the application of horizontal seismic bands. *Engineering Structures,* 283**,** 115897.